

# The SPEX Speaker

INDUSTRIES, INC. - 3400 PARK AVENUE - METUCHEN, N.J. 08840 - TEL: 201-549-7144

## FOCUSING ON LENSES WITH LASER RAMAN SPECTROSCOPY

Nai-Teng Yu

School of Chemistry, Georgia Institute of Technology, Atlanta, GA 30332

and

John F.R. Kuck, Jr.

Department of Ophthalmology, Emory University, Atlanta, GA 30322

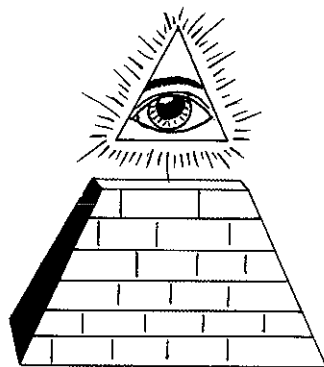


Fig 1 in a highly schematic fashion in which dimensional changes are exaggerated. The sphincter is shown in cross section so the elongated triangle represents the contracted state although it may appear otherwise. The capsule is an elastic bag of collagenous tissue totally enclosing the mass of lens fibers and molding the shape of the lens as external force is applied to the capsule. This molding is possible because the fibers have some capacity to change their shape

and to slide past one another.

In some fish, focusing is accomplished entirely by lens movement along the visual axis. In the cormorant, a bird which must focus both in air and under water, the variability of lens strength amounts to 30 diopters as compared to a mean value of 14 diopters in a child. It is worth noting that bird lenses are very soft compared with mammalian lenses, while fish lenses are usually very hard with a high proportion of protein

The ocular lens is a remarkably transparent organ containing a large proportion of protein to give a high index of refraction and having a structure which satisfies the requirements of transparency, capacity to change its shape, and ability to maintain its properties by metabolic processes. Most of the eye's refraction occurs at the cornea-air interface because here lies the greatest difference in refractive index. The refraction of the lens is important, however, not because of its small contribution to total eye refraction, but because its contribution is variable, allowing the image to be focused on the retina whether it comes from a scene at an infinite distance or only half an arm's length away.

The eye focuses on an object nearer than about 5 meters by a process called accommodation in which the lens becomes thicker than in the unaccommodated state. The mechanism involves both a contraction of a sphincter called the ciliary muscle and the resulting increase in slack of the zonule that no longer transmits the tension of the muscle to the lens capsule at the equator. These two states of the lens are shown in

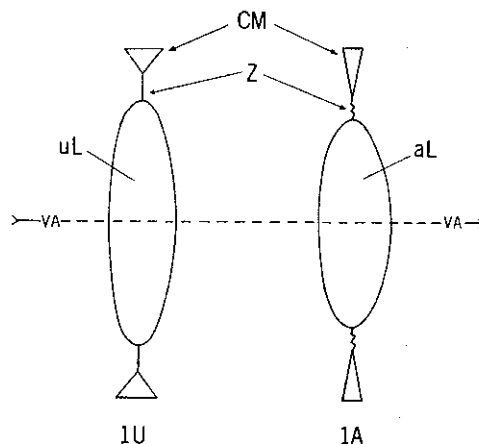


Fig 1 The lens is suspended in the visual axis VA by a circular ligament called the zonule Z which in turn is anchored to the inner eyeball by a circular sphincter, the ciliary muscle CM. In the unaccommodated lens uL, set for far vision, the ciliary muscle is relaxed (Fig 1U), the zonule is under tension and therefore stretches the lens capsule and its contents into a flatter shape. In accommodation (Fig 1A) the ciliary muscle contracts, forming a smaller ring which allows the zonule within it to become slack. Relaxed from zonule tension, the capsule also relaxes and assumes a more spherical shape, as does the fiber mass of the lens itself. This thicker lens aL has more magnifying power and brings the image of a near object into focus on the retina. Variable focusing is the primary function of the lens and all its properties are adapted to this purpose.

Lenses found in nature exhibit an astounding diversity of adaptations<sup>2</sup>, ranging from the mobile scanning lens of the copepods (Fig 2)<sup>3,4</sup> to the stationary lenses in the leaves of some tropical plants, that gather the dim light of the rain forest and concentrate it on the chloroplasts<sup>5</sup>. The evolutionary pressure which has been so efficient in fitting every light-sensitive organism with a system perfectly adapted to its needs has, however, failed in at least one instance for the human organism. Man now has a life span extending far beyond the breeding age. Thus, any defect in the lens which develops beyond middle age will not affect reproductive behavior and therefore cannot be bred out of the population.

Senile cataract is such a defect; and since it is one of the major causes of blindness in older people there is great interest in research which will lighten this burden by prevention, palliative treatment, or cure. At present, lens research is still accumulating the basic knowledge needed to attack the problem of normal lens metabolism and what goes wrong to cause cataracts. The essential solid constituent of the lens is the refractile protein. Therefore much work has centered on gaining an understanding of the proteins (or crystallins), which are unique to the lens and are otherwise rather unusual. It has often been assumed that some malfunction involving the lens proteins is the key to cataract formation.

#### Protein Composition of the Lens<sup>6</sup>

The lens proteins of all mammalian species are similar and may be separated by chromatography into three water-soluble fractions:  $\alpha$ -,  $\beta$ -, and  $\gamma$ -crystallin. The water-insoluble fraction, separated by centrifugation, is called albuminoid. The  $\alpha$ -crystallin fraction, which has the highest molecular weight ( $\sim 1 \times 10^6$  daltons or greater), is composed of four different subunits labeled A<sub>1</sub>, A<sub>2</sub>, B<sub>1</sub> and B<sub>2</sub>. These subunits have molecular weights of approximately 20,000 daltons. The  $\beta$ -crystallins, somewhat smaller than the  $\alpha$ -crystallins, are normally considered as a group of proteins of variable size ranging from 24,000 to 35,000 daltons. The  $\gamma$ -crystallins, the smallest of the crystallins (molecular weight  $\sim 1.7 \times 10^4$  daltons), contain high levels of sulfhydryl and tryptophan. The nucleus of the lens is normally richer in  $\gamma$ -crystallin, when compared to the outer region (cortex). Bovine  $\gamma$ -crystallin (fraction II) was recently crystallized<sup>7</sup>.

The lenses of birds and reptiles contain a unique protein called  $\delta$ -crystallin, which is absent in the mammalian lens. The  $\delta$ -crystallin, the replacement of  $\gamma$ -crystallin in mammalian lenses, is very low in sulfhydryl and tryptophan, the two groups which have been repeatedly implicated in human senile nuclear cataract<sup>8-11</sup>.

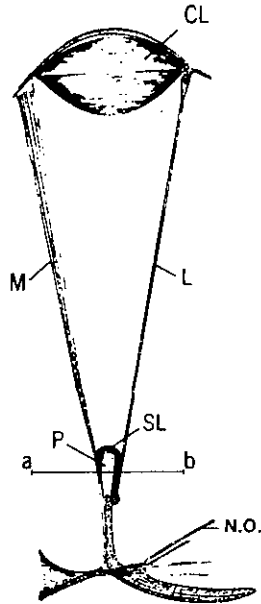


**Fig 2** The scanning lens is possessed only by female copepods. The anterior corneal lens CL (.15 mm dia.) is attached to the carapace of the small crustacean. CL is connected to the posterior scanning lens SL (.03 mm dia.) by a system of muscles and ligaments forming a delicate cone-shaped membrane. In the diagram only one ligament L and one muscle bundle M are shown in the plane of the paper. A series of these elements spaced around the peripheries of the lenses make up the membranous cone. The scanning lens SL is an inverted U-shaped structure which caps the conical, heavily pigmented photosensitive element P nestled in the apex of the membranous cone and from it leads the optic nerve N.O. The scanning lens is in continual movement along the axis a-b at a maximum scan rate of 5 per second; the amplitude of the scan is about 4x the lens diameter.

Interestingly enough, the bird lens is known to have a low incidence of cataracts<sup>6</sup>.

#### What are Cataracts?

There is no universally acceptable answer to this question since some prefer to include in the definition lenses which contain a high enough concentration of transparent pigment to impair vision. Lenses of this type, which can transmit a dim image if the object seen is bright enough, we shall exclude. A cataract then is a lens containing optical discontinuities which scatter enough light to interfere appreciably with vision acuity. Since any sufficient insult to the lens produces a cataract, it is obviously not a single entity and the term properly should be used in the plural.

There appear to be four rather distinct types of cataracts: 1) the occurrence of zones having a significantly lower refractive index than healthy fibers causes light scatter at the interfaces between these zones and the fibers. Such zones (water clefts, vacuoles, etc.) are generally extracellular. Many senile cortical cataracts belong in this group. 2) the accumulation of dispersed protein molecules of sufficient size and concentration produces a Tyndall scattering inside the lens fibers. Nuclear senile cataracts are of this type according to some investigators. 3) the binding of high molecular weight protein to plasma membranes may give interfaces which scatter light. More mature senile cortical cataracts exhibit this change in addition to the changes found in type 1. 4) all cataracts not belonging to 1, 2, or 3 are included in this highly heterogeneous group. The accumulation of particles (calcium oxalate, cholesterol, lipid, cell debris, etc.) of microscopically visible size causes serious light scattering. Faulty protein synthesis due to genetic defects can also result in light scattering zones.

#### What Causes Cataracts?

The causes of cataracts are many but the situation can be analyzed from a simplistic viewpoint which may aid in understanding cataractogenesis. The energy expended by the lens serves two purposes: 1) the maintenance of water and ionic balance between the lens cell (high in potassium and protein; low in sodium) and the two humors (low in potassium and protein; high in sodium) which surround it; 2) the synthesis of protein and the transport into the lens cell of the amino acids necessary for such synthesis. The greater part of the work done serves the first purpose and we may expect any interference with water-ion balance to produce opacity. Failure of energy-producing metabolic processes and failure to maintain membrane integrity are the two basic reasons for the development of a large class of cataracts which is characterized by osmotic or ionic imbalance, the formation of extracellular vacuoles, and lens swelling. Another, and probably less important, class of cataracts is characterized by abnormal protein synthesis caused by genetic defects or metabolic insults such as those imposed by certain anti-metabolites, photo-oxidation, or the activation of proteases. In summary, any process which perturbs the short range homogeneity of the refractive index of the lens will cause light scattering. Thus cataracts are the result of a large number of quite different processes ranging from the purely physical trauma of the accommodative action (as proposed by Fisher<sup>12</sup>) to the osmotic effect of sugar alcohols accumulating in the diabetic lens<sup>9</sup>.

#### Cataract Research: Purpose and Methods

The purpose of cataract research is to understand the normal processes that maintain the clarity of the lens so pathological processes leading to opacity may be controlled or prevented. Cataracts from humans or experimental animals may be analyzed to determine the biochemical

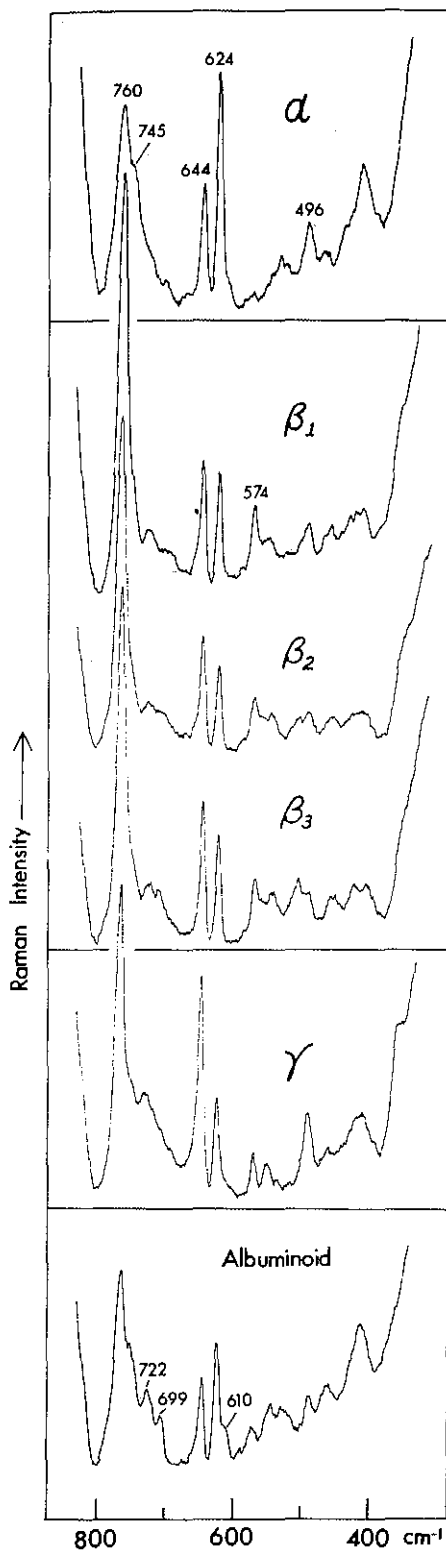


**Fig 3** Raman spectra ( $300-800\text{ cm}^{-1}$ ) of bovine lens crystallins ( $\alpha$ ,  $\beta_1$ ,  $\beta_2$ ,  $\beta_3$  and  $\gamma$ ) and albuminoid in freeze-dried powder form. Reproduced from *J. Biol. Chem.*, 250, 2196 (1975). The spectra were obtained with the 514.5 nm line excitation and about  $4\text{ cm}^{-1}$  spectral slit-width resolution. The laser power at the sample was approximately 80 milliwatts.

changes associated with the cataract. Normal lenses may also be incubated under various conditions to see what alterations occur in the lenses. Raman spectroscopy is a highly useful tool for both these types of studies<sup>13-16</sup>. It is especially valuable as a non-invasive, non-destructive probe for an intact, living lens maintained in a highly physiological state in an organ culture procedure. An advantage of Raman in lens research is that the narrow laser beam allows analysis of a very small zone of the lens (optical dissection so to speak). Such an analysis implies the ability to carry out an aging study since a lens has within it all the substances from its complete history, beginning with the nucleus which represents the fetal lens, to the outer cortex which consists of the youngest fibers. A recent finding of great importance and possible only by Raman spectroscopy is that the young bird lens, which is cataract resistant, has a high proportion of a specific protein existing in the  $\alpha$ -helical conformation<sup>15,16</sup>. In contrast, the proteins of all mammalian species examined occur only in the  $\beta$ -pleated sheet conformation<sup>13,15,16</sup>. It was also shown<sup>16</sup> that the heat-induced conversion of the  $\alpha$ -helix to the  $\beta$ -pleated sheet occurred simultaneously with opacification.

#### Application of Raman Spectroscopy to Crystallins and Intact Lenses

(I) Raman spectra of  $\alpha$ -,  $\beta$ -,  $\gamma$ -,  $\delta$ -crystallin and albuminoid.

Raman spectroscopic studies of isolated lens proteins were first carried out by Yu and East<sup>13</sup>. The water-soluble proteins of the bovine lens were separated on a column of Sephadex G-200 into five fractions labeled as  $\alpha$ -,  $\beta_1$ -,  $\beta_2$ -,  $\beta_3$ -, and  $\gamma$ -crystallin. In the low wavenumber region ( $300-800\text{ cm}^{-1}$ , Fig 3) the aromatic side groups phenylalanine (Phe), tyrosine (Tyr), and tryptophan (Trp) give rise to intense Raman lines at 624, 644, and  $760\text{ cm}^{-1}$ , respectively. The Tyr/Phe ratio is similar for the three subfractions of the  $\beta$ -crystallin, but quite different from those of  $\alpha$ - and  $\gamma$ -crystallin. The  $\alpha$ -crystallin is high in Phe and low in Tyr, but  $\gamma$ -crystallin is low in Phe and high in Tyr. The spectrum of albuminoid, similar to that of  $\alpha$ -crystallin, suggests that the water-insoluble fraction may be derived from  $\alpha$ -crystallin in bovine lens. However, a similar study<sup>17</sup> on isolated rat lens proteins indicates that rat albuminoid is closely related to  $\gamma$ -crystallin. In the  $2500-2800\text{ cm}^{-1}$  region, the protein sulphhydryl groups exhibit strong Raman lines at  $2582\text{ cm}^{-1}$  (Fig 4), due to S-H stretching vibrations. The  $\gamma$ -crystallin has the highest intensity at  $2582\text{ cm}^{-1}$ , indicating that nearly all the -SH groups in  $\gamma$ -crystallin remain in the reduced form after

chromatographic separation. The absence of the disulfide formation in  $\gamma$ -crystallin is indicated by the absence of a Raman line near  $508\text{ cm}^{-1}$  (see Fig 3). The increasing intensity at this wavenumber in  $\beta_1$ ,  $\beta_2$  and  $\beta_3$  spectra provides evidence that substantial numbers of disulfide bonds were formed in isolated  $\beta$ -crystallins. It is apparent that the -SH groups in the  $\beta$  fractions can be readily oxidized, while those of the  $\gamma$ -crystallins are oxidation-resistant.

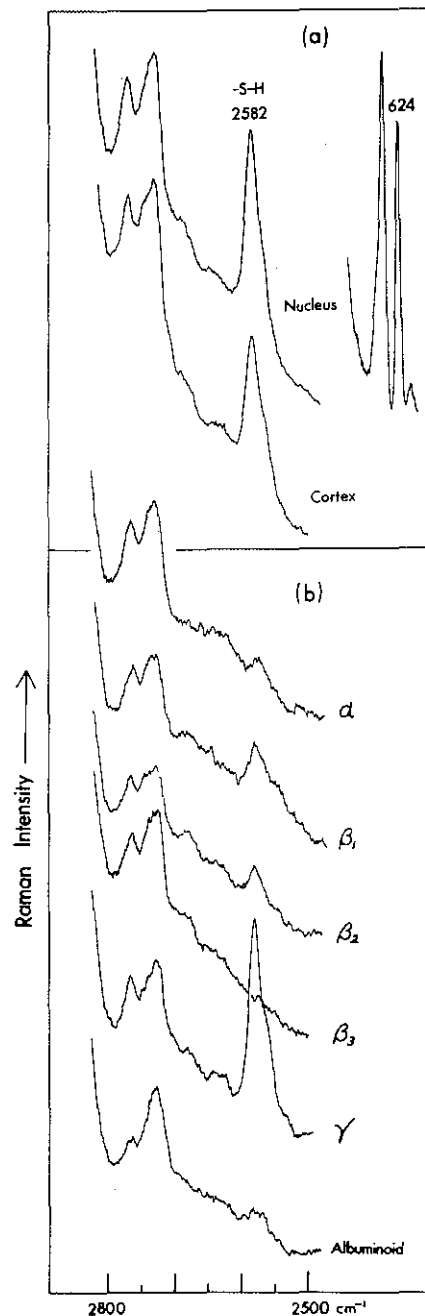


**Fig 4** Raman spectra of bovine lens and its isolated crystallins in the  $2500\text{ to }2800\text{ cm}^{-1}$  region showing scattering from the -SH groups. Reproduced from *J. Biol. Chem.*, 250, 2196 (1975).

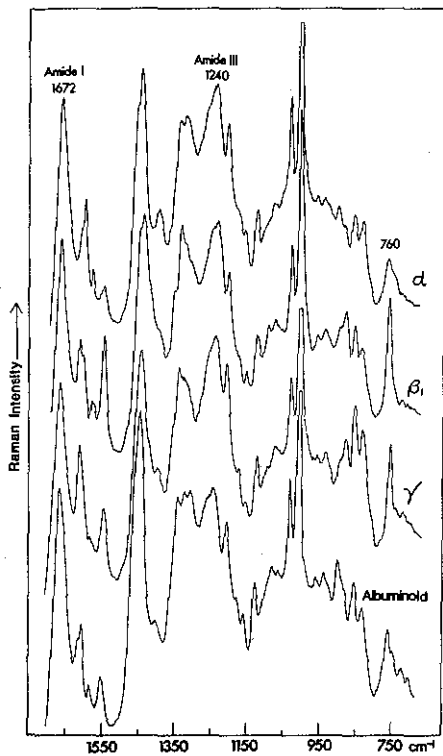


Fig 5 Raman spectra of  $\alpha$ ,  $\beta_1$ ,  $\gamma$  and albuminoid (freeze-dried powder) showing amide I and amide III regions. Reproduced from J. Biol. Chem. 250, 2196 (1975).

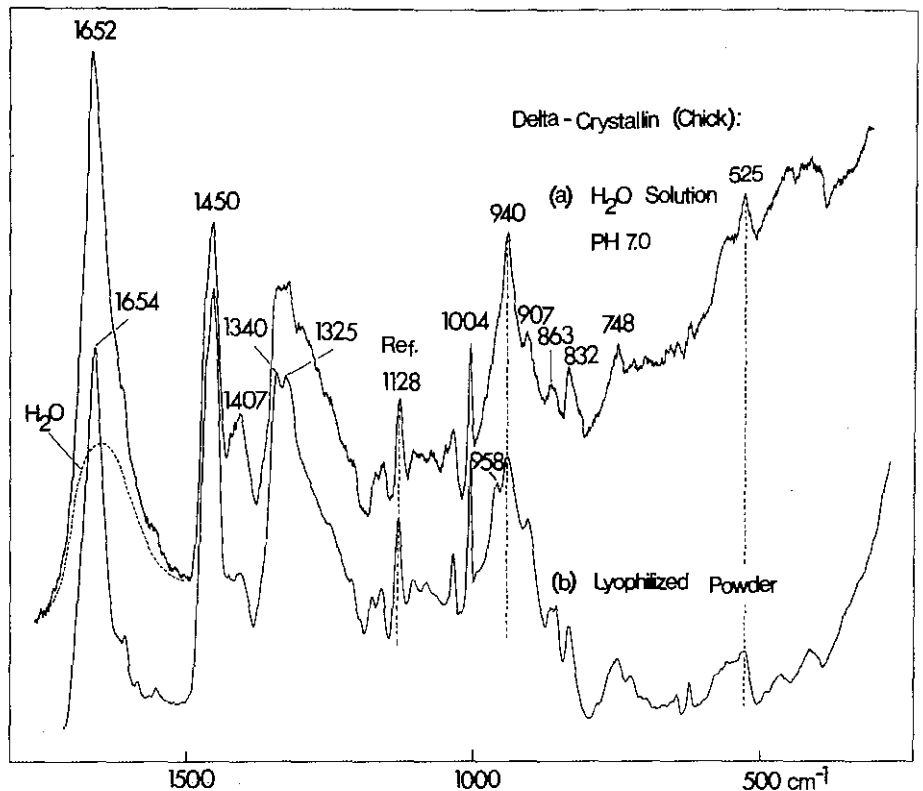


Fig 6 Raman spectra of  $\delta$ -crystallin in  $\text{H}_2\text{O}$  (pH 7.0) and freeze-dried state. The  $\delta$ -crystallin was isolated from chick lens. The strong amide I vibration at 1652  $\text{cm}^{-1}$  and the absence of a strong amide III at 1240  $\text{cm}^{-1}$  are the indication of  $\alpha$ -helical conformation. Reproduced from Exp. Eye Res. 24, 321 (1977).

The polypeptide backbone conformation of  $\alpha$ -,  $\beta$ - and  $\gamma$ -crystallin is seen in the so-called amide I (1650-1680  $\text{cm}^{-1}$ ) and amide III (1220-1300  $\text{cm}^{-1}$ ) regions. Studies<sup>18-22</sup> of the Raman spectra of synthetic polypeptides and proteins of known structure indicate that the  $\alpha$ -helical form displays a strong amide I line at  $1650 \pm 5 \text{ cm}^{-1}$ , with relatively weak scattering in the amide III region, and that anti-parallel  $\beta$ -pleated sheet gives a strong and sharp amide I at  $1670 \pm 2 \text{ cm}^{-1}$  with a strong amide III line near 1240  $\text{cm}^{-1}$ . The random-coiled form<sup>23</sup>, on the other hand, shows a broad amide I line at  $\sim 1665 \text{ cm}^{-1}$  with a medium intensity, but broad amide III at  $\sim 1248 \text{ cm}^{-1}$ . With this information, the examination of the spectra of  $\alpha$ -,  $\beta_1$ -,  $\gamma$  and albuminoid shown in Fig 5 demonstrates that these isolated proteins are mainly anti-parallel  $\beta$ -pleated sheet structures. More interesting is the discovery of  $\alpha$ -helical conformation<sup>15,16</sup> in chick-lens  $\delta$ -crystallin. The Raman spectra presented in Fig 6 show clearly, in the amide I and amide III regions, that the isolated  $\delta$ -crystallin in both solution and lyophilized (freeze-dried) powder exists predominately in the  $\alpha$ -helical form. This same conclusion was reached by the circular dichroism

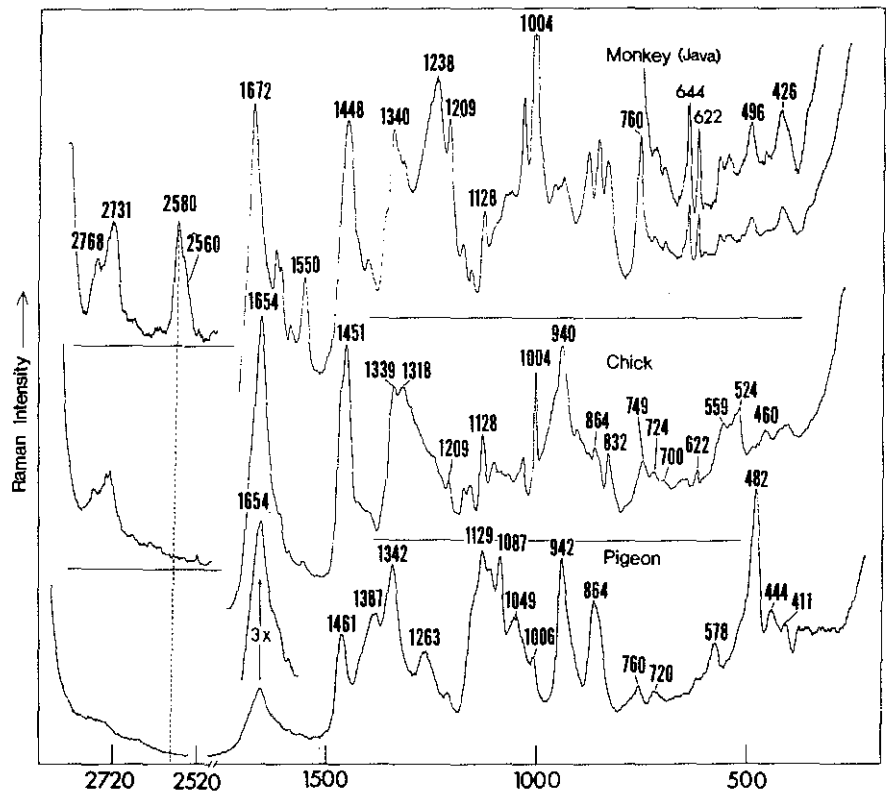


Fig 7 Comparison of the Raman spectra of monkey (Java,  $\sim 3$  years old), chick ( $\sim 10$  days) and pigeon ( $\sim 8$  weeks). Raman signals were obtained from the center of the lens. The difference noted at 2580  $\text{cm}^{-1}$  (S-H stretching vibration) is quite striking. Reproduced from Exp. Eye Res. 24, 321 (1977).

studies<sup>16,24</sup>. Both Raman<sup>16</sup> and circular dichroism<sup>16,24</sup> studies gave an estimate of approximately 75%  $\alpha$ -helix. In agreement with the previous biochemical analysis, Raman data indicate very low levels of SH (not shown) and tryptophan (weak intensity at 1550  $\text{cm}^{-1}$ , Fig 6) in  $\delta$ -crystallin.

(II) Raman studies of intact human and animal lenses.

The most exciting information obtained by Raman spectroscopy of the lens pertains to protein conformation in the intact, living lens<sup>13-17</sup>. This organ offers a unique system for examination by Raman spectroscopy because it is nearly perfectly transparent and because it contains a high enough concentration of protein (30%) to give a Raman emission significantly above background. Since the lens lacks blood vessels and nerves, it is normally in a state resembling cells in a culture. It is immersed in two media, the aqueous and vitreous humors, which supply its nutrients and remove its metabolic products—the same sort of role a medium plays in a cell culture. Thus, a lens removed from an animal can survive in a highly physiological state under conditions which are ideal for irradiating it with a laser beam and measuring the Raman emission. With this technique it has been shown<sup>15,16</sup> that all young bird and reptile lenses have their characteristic protein,  $\delta$ -crystallin, in the  $\alpha$ -helical form. In contrast, the vertebrate lens proteins exist chiefly in the  $\beta$ -pleated sheet<sup>13-16</sup>. This unusual feature of the bird lens has been suggested as the basis for other properties such as its soft texture, its failure to develop a hard nucleus on aging, and its high proportion of water as compared with other lenses. Even more important is a possible connection between the preponderance of  $\alpha$ -helical protein and the apparent freedom from cataract formation in the bird lens.

In addition to the presence of the  $\alpha$ -helix, lenses of flying birds are characterized by the presence in the nucleus of a remarkably high concentration of glycogen (5%) which appears to be a virtual substitute for  $\gamma$ -crystallin, the chief nuclear protein in most vertebrate lenses. Glycogen has a distinct advantage over protein since it does not contain amino acids prone to degradation (including cross linking and discoloration). Thus birds, which are nearly always diurnal, are not affected by the ultraviolet component of sunlight. Another property of lens glycogen which is a complete mystery is how such an insoluble molecule is maintained in a state of perfect clarity in the lens although even a dilute glycogen solution in pure water is opalescent. The lens of a pigeon nestling develops a blue haze in the nucleus on chilling, resembling the "cold cataract" of very young mammals.

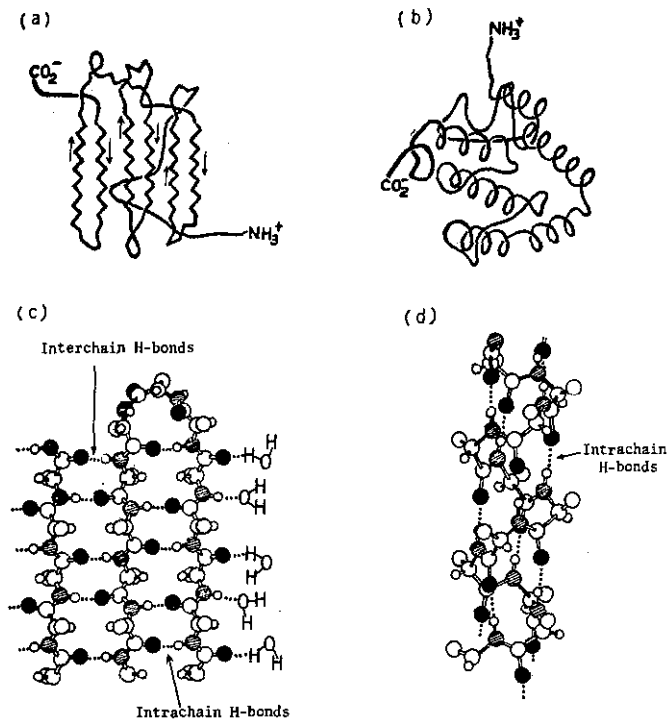


**Fig 8** Schematic representation of a globular protein having predominantly anti-parallel  $\beta$ -pleated sheet conformation (a) or  $\alpha$ -helical conformation (b). Detailed structure of the two conformations is shown in (c) and (d). The polypeptide chain of  $\beta$ -conformation is capable of forming hydrogen bonds within the same chain (intrachain H-bonds), between different chains (interchain H-bonds) or with water molecules. The peptide units in  $\alpha$ -helical conformation form only intrachain H-bonds.

Although there was already firm evidence for the occurrence of glycogen in the nucleus of certain bird lenses (notably those belonging to families of flying habit), this feature was strikingly apparent in a comparison of Raman spectra (Fig 7) from a chicken (ground runner) and a pigeon (flyer). Many glycogen bands are visible; those at 482, 864, 942, 1087, 1129, 1342, 1387 and 1461  $\text{cm}^{-1}$  do not correspond to any bands in the chick lens spectrum.

Duke-Elder<sup>29</sup> has expressed the opinion that the vertebrate eye is at the evolutionary peak in birds. The avian lens has several unusual properties which appear to be associated with the superior vision legendary in birds. A bird of prey can distinguish a potential victim at a great distance yet the lens must accommodate so well that the strike is accurate enough to be fatal. This capacity for rapid and wide-ranging accommodation depends on the ease of lens deformation. The bird lens is much softer than that of mammals or fish. Although the consistency may be due in large part to the high proportion of water (about 80% as compared to 65% for the rat lens), another contributing factor is the presence in bird lenses (and reptile lenses) of a unique protein,  $\delta$ -crystallin, which exists in the  $\alpha$ -helical conformation. All other lens proteins have the  $\beta$ -conformation which leads to a firmer 3-dimensional structure because of interchain hydrogen

bonding. As shown in Fig 8, the two conformations have fine structures which lead to a difference in the degree of compactness. The  $\alpha$ -helix has the coils in close apposition so that there is a strong tendency for the formation of intrachain hydrogen bonding between adjacent peptide units of the same molecule. This not only leads to a tight-coiled structure, but decreases the tendency for the formation of interchain bonds characteristic of the  $\beta$ -conformation. Furthermore, the backbone chain in the  $\alpha$ -helix does not form hydrogen bonds with water, so the water surrounding it is more fluid than the bound water found tightly associated with the  $\beta$ -conformation. The final result of this difference in conformation and its effect on lens water is to give a structure of lower consistency when the alpha-helix is predominant. Thus the soft lens of the bird is an ideal object for the forces which deform it. Strangely enough, bird lenses (and reptile lenses) do not have the zonule-ciliary muscle apparatus for lens deformation, only a ciliary muscle. Accommodation is accomplished by a mechanism which is not well understood but involves pressure on the lens from the ciliary muscle and perhaps even some capacity of the lens itself for changing its shape.

It has long been known that all vertebrate lenses have highly similar protein compositions. The usual explanation for this is that the lens developed rather early in vertebrate evolution in some remote ancestor whose identity is not clear. At that time the lens was shut off from the rest of the body by the capsule, a membrane impermeable to protein molecules. Thus the opportunity for further evolutionary changes was reduced. Those changes which have occurred are mostly so subtle that they are detectable only by immunological means. The relationships are so widespread, crossing both generic and species borders, that those in the field say that lenticular proteins are organ-specific not species-specific. Differences that do exist between lenses depend on rather superficial and minute changes in protein composition and conformation and do not affect the Raman spectrum of the lens. However, the age-related increase in the synthesis of  $\alpha$ -crystallin (high in phenylalanine, low in tyrosine) accompanied by decreased synthesis of  $\gamma$ -crystallin (low in phenylalanine, high in tyrosine) are changes readily apparent in Raman spectra<sup>26</sup>.

Raman spectra of an old hen lens (~10 years)<sup>16</sup>, obtained from the nucleus, intermediate zone, and cortex, are shown in Fig 9. The advantage of Raman spectroscopy demonstrated here is that the small size of the laser beam allows excitation of a small zone and collection of the signal from an even smaller part of that zone. A typical scattering volume is only  $1 \times 10^{-9} \mu^3$ !! This fact is of special interest to researchers because different parts of the lens represent structural material synthesized at a particular time in the animal's life and not greatly modified after that. The nucleus of the lens is the vestige of the fetal lens, while the outer part (cortex) just under the capsule is the most recently formed. Thus, it becomes possible to study in a single sample some of the effects of aging, a most important facet of research on senile cataract. The structural information reflected in Fig 9 is quite illuminating. First, it clearly shows that the proteins in the nuclear region are different from the proteins in the cortical region in both composition and conformation. There is a conformational transition from  $\alpha$ -helix to  $\beta$ -conformation in going from nucleus to cortex. The Raman spectrum of the old hen nucleus (spectrum (a) of Fig 9) is identical to that of the nucleus of the lens of a 10-day-old chick, indicating that the  $\delta$ -crystallin does not change its  $\alpha$ -helical conformation in the aging process. Secondly, the Raman spectrum of the old hen lens cortex is similar to that of the bovine lens (cortex or nucleus, Figs 4 and 10). The relative intensities of the Raman lines at 624 (Phe), 644 (Tyr) and 1550 (Trp)  $\text{cm}^{-1}$  indicate that the proteins of the hen lens cortex have approximately the same

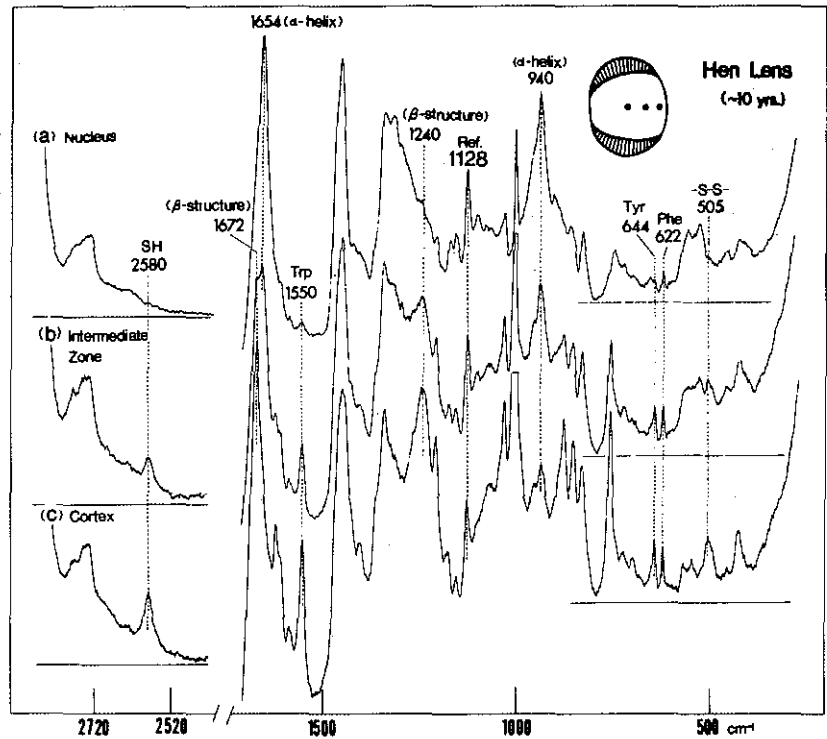


**Fig 9** Raman spectra of a 10-year-old hen lens. Spectra were obtained from three different spots in the intact lens, as indicated in the diagram. The spectra in the 2500-2800  $\text{cm}^{-1}$  region were recorded at 5 times greater sensitivity than that for the 300-1800  $\text{cm}^{-1}$  region. Reproduced from *Exp. Eye Res.* 24, 321 (1977).

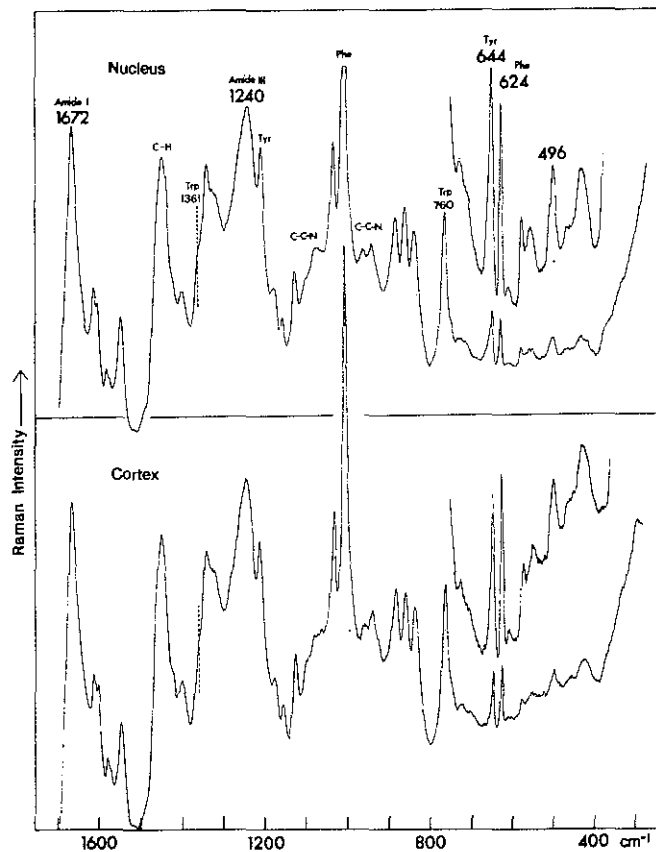


**Fig 10** Raman spectra of intact bovine lens (~3 yrs.). A laser power of 150 milliwatts was used to generate the spectra. Spectral features are not sensitive to location except the relative intensities at 624 and 644  $\text{cm}^{-1}$ . Reproduced from *J. Biol. Chem.* 250, 2196 (1975).

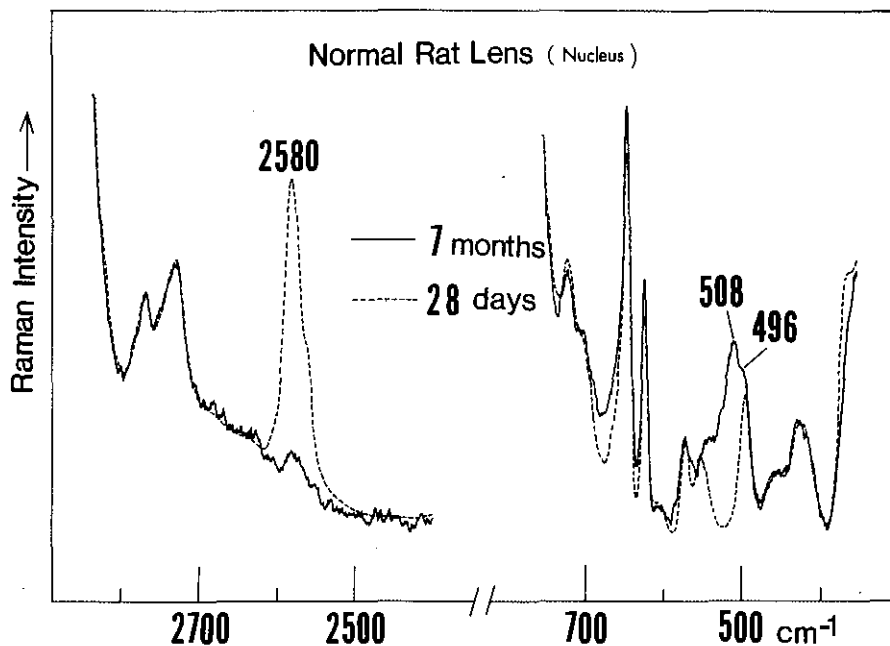


Fig 11 Raman spectra in the -SH and S-S vibrational regions of intact rat lens (nucleus, 28 days and 7 months old) showing striking age effect. Reproduced from J. Biol. Chem. 253, 1436 (1978).

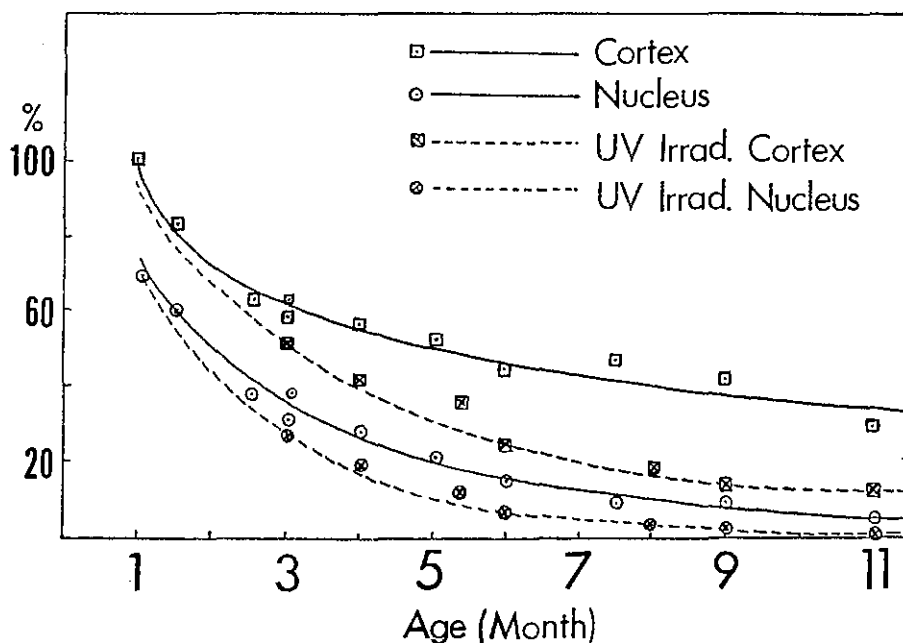


Fig 12 Effect of UV irradiation on total % -SH in a mouse lens as a function of age. The Raman intensity at  $2580 \text{ cm}^{-1}$  was measured from both cortex and nucleus regions. The radiation source (General Electric F-15T8 BLB UV lamp) had a spectral distribution in the 300 to 400 nm region with its maximum at  $\sim 353 \text{ nm}$ . The power density at the lamp surface was about 4 milliwatts/ $\text{cm}^2$ . Mice were placed in plastic cages for continuous UV irradiation after weaning at about 1 month of age. The mice were able to tolerate this relatively low intensity UV light without closing their eyes. Reproduced from J. Biol. Chem. 253, 1436 (1978).

aromatic amino acid content as the bovine lens crystallins. The strong amide I line at  $1672 \text{ cm}^{-1}$  and the amide III at  $1240 \text{ cm}^{-1}$  indicate that these proteins are mostly in the antiparallel  $\beta$ -sheet conformation as all bovine lens crystallins are. The striking differences among the spectra of monkey, chick, and pigeon lenses are indicated in Fig 7.

Among the few non-aromatic groups which give a detectable Raman signal are SH and S-S groups. This is most fortunate since both the concentration and state of the sulfur in the lens have always been of great interest with respect to age-induced changes and alterations associated with cataract formation. It has been possible<sup>26</sup>, for instance, to follow the changes of SH and S-S in the aging rat or mouse lens and in the lenses of mice exposed to long-wave ultraviolet (peak at  $353 \text{ nm}$ ) for several months, a procedure which ultimately produces cataracts. To illustrate the dramatic spectral changes as a result of aging, Raman spectra of a 28-day-old and a 7-month-old rat lens nucleus are presented in Fig 11. The decrease in intensity of the  $2580 \text{ cm}^{-1}$  line (attributed to sulfhydryl) along with the increase in intensity of the  $508 \text{ cm}^{-1}$  (attributed to disulfide bond stretching vibration) is unequivocal evidence that most of the thiol groups of lens proteins have been converted to disulfide bonds before 7 months of age (20% of the life expectancy). One effect of long wave ultraviolet light on lens proteins can be readily detected by Raman spectroscopy. Fig 12 shows that exposure of mice to long-wave UV irradiation *in vivo* accelerates the normal disappearance of lens sulfhydryl groups with aging.

An interesting facet of the problem of lens sulfur is the accessibility of SH groups to oxidation and other reactions, since this is a limitation on the reactivity of SH. The Raman technique has a particularly valuable application<sup>26</sup> in this instance because the H of SH will exchange with the D of  $\text{D}_2\text{O}$ , forming an SD group which gives a Raman signal distinctly different from that given by SH. The exchange is reversible, fairly rapid, and is carried out under ideal conditions for maintaining the lens in a physiological state. The deuterium exchange studies<sup>26</sup> on the rat lens indicate that the majority of the sulfhydryl groups in the nucleus are exposed to water up to the age of 4 months. Disulfide linkages are formed and the amount and percentage of exposed -SH groups drop linearly as the lens ages.

At present, the most serious shortcoming of Raman spectroscopy in cataract research is that all cataractous changes produce an intolerable level of Tyndall scattering which makes measurement of Raman scattering impossible. Raman intensities are seriously attenuated by partially opaque regions and thus signals are difficult to extract even by

the photomultiplier-photon counting (PMT-PC) detection technique. Recent advances in the use of a Silicon Intensified Target-Optical Multichannel Analyzer for Raman spectroscopy<sup>27</sup> indicate that it is possible to obtain high-quality Raman spectra of an intact lens with a very low laser power ( $\sim 1$  mW). When opacities are present, higher power will produce a detectable signal in spite of the attenuation. New SIT-OMA Raman techniques open up the field for systematic structural studies of both naturally occurring and experimentally induced cataracts. The Raman probe, if directly applied to human or animal eyes, may be a very useful tool for detecting precataractous changes or for monitoring the development of cataract formation induced by drugs or radiation.

Another shortcoming of Raman spectroscopy for lens research is fluorescent interference from pigments accumulated in human lenses and a few other species of lenses during aging. However, the fluorescent background can be greatly reduced with long wavelength excitation. For example, Raman spectra of a human lens younger than 1 year of age can be obtained with excitation at 457.9 nm, but those of a 7-year-old lens are obtainable only with excitation at 514.5 nm or longer wavelengths. It was recently demonstrated in our laboratory that a 23 year old human lens had a strong fluorescent emission with its maximum at 556.4 nm when excited at 514.5 nm and thus Raman spectra were not obtainable at this or shorter wavelengths. With longer wavelength excitation at 600 nm, generated by a pulsed dye laser, satisfactory Raman spectra of this human lens have been obtained (Fig 13).

Several techniques are available to suppress or avoid a fluorescent background. These include phase detection with a rotating polarizer<sup>28</sup>, pulsed laser excitation with gated detectors<sup>29</sup>, or nonlinear processes such as coherent anti-Stokes Raman scattering (CARS)<sup>30,31</sup>, Raman-induced Kerr effect spectroscopy (RIKES)<sup>32-34</sup>, or the inverse Raman effect<sup>35,36</sup>. The CARS technique has been demonstrated<sup>30,31</sup> to be quite effective in discrimination against fluorescence. However, it cannot be applied to the eyes of living animals or humans because of the requirement of two crossed beams and the generation of a third beam in the forward direction. A gated SIT-OMA detection method should offer the possibility of clinical Raman applications with a capability for fluorescence discrimination.

#### Acknowledgements

Our research in Raman spectroscopy of intact lenses has been supported by grants from the National Eye Institute (EY 01746 and EY 00260). N.T. Yu is a recipient of a

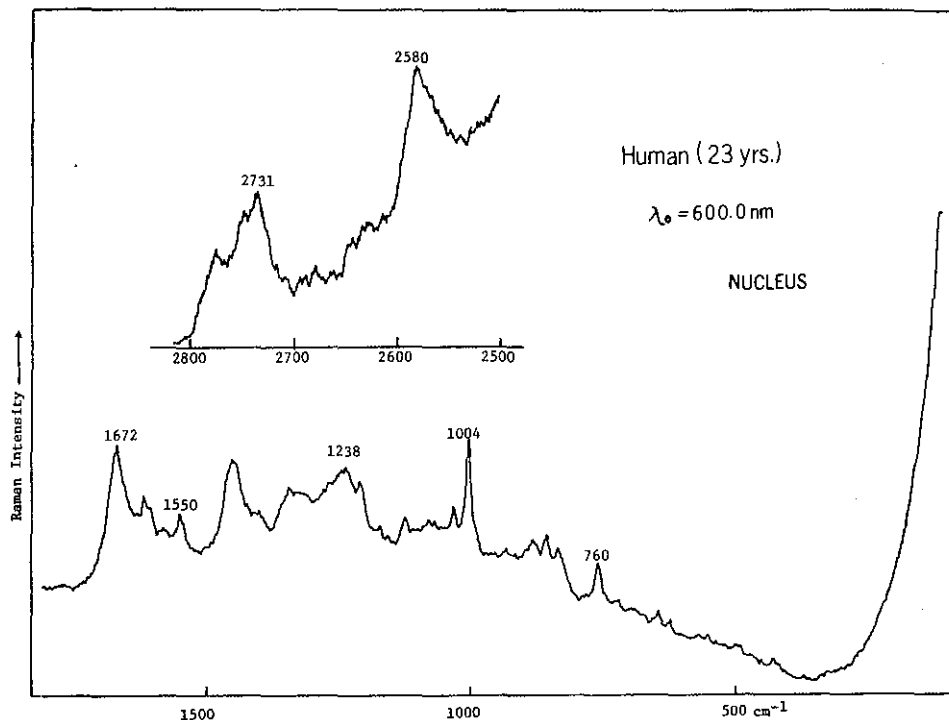


**Fig 13** Raman spectrum of a 23-year-old human lens (nucleus) with 600.0 nm excitation. The laser power at the sample is  $\sim 100$  mW and the spectral slit width  $\sim 5$  cm<sup>-1</sup>. The pulsed laser (1  $\mu$  second pulse width) was operated at 30 Hz.

National Eye Institute Research Career Development Award (EY 00073). Human lenses were from donor eyes contributed by the Atlanta Lions Eye Bank.

#### References\*

- R. Moses, "Adlers Physiology of the Eye", Chapter 10, p. 350-371, 5th edition, C.V. Mosby, St. Louis 1970.
- G.L. Walls, "The Vertebrate Eye and its Adaptative Radiation", Cranbrook Institute of Science, Bloomfield, Michigan, 1942.
- R.L. Gregory and H.E. Ross, *Nature* **201**, 1166 (1964).
- S. Exner, "Physiology of the Faceted Eyes of Crustacea and Insecta", Fig. 22, p. 136 (1891). Franz Deuticke, Leipzig and Wein.
- Life Magazine*, Vol. 61, December 23, 1966.
- J.F.R. Kuck, Jr., in "Cataract and Abnormalities of the Lens (J.R. Bellows Ed.), Chapter 3, pp. 69-96, Grune and Stratton, Inc. New York, N.Y. 1974.
- C.H. Carlisle, P.F. Lindley, D.S. Moss and C. Slingsby, *J. Mol. Biol.* **110**, 417 (1977)
- J.F.R. Kuck, Jr., in "Biochemistry of the Eye" (C.N. Graymore Ed.), Chapter 5, Academic Press, New York, N.Y. 1970. Also references cited therein.
- E.I. Anderson and A. Spector, *Exp. Eye Res.* **26**, 407 (1978).
- J.J. Weiter and E.D. Finch, *Nature*, **254**, 536 (1975).
- R.J.W. Truscott and R.C. Augusteyn, *Exp. Eye Res.* **24**, 159 (1977).
- R.F. Fisher, *Exp. Eye Res.* **16**, 41 (1973).
- N.T. Yu and E.J. East, *J. Biol. Chem.* **250**, 2196 (1975).
- R.A. Schachar and S.A. Solin, *Invest. Ophthalmol.* **14**, 380 (1975).
- J.F.R. Kuck, Jr., E.J. East and N.T. Yu, *Exp. Eye Res.* **22**, 9 (1976).
- N.T. Yu, E.J. East, R.C.C. Chang and J.F.R. Kuck, Jr., *Exp. Eye Res.* **24**, 321 (1977).
- R.C.C. Chang, Ph.D. Thesis, Georgia Institute of Technology, Atlanta, Ga. 1976.
- T.J. Yu, J.L. Lippert and W.L. Peticolas, *Biopolymers*, **12**, 2161 (1973).
- M. C. Chen and R.C. Lord, *J. Amer. Chem. Soc.* **96**, 4750 (1974).
- B.G. Frushour and J.L. Koenig, *Biopolymers*, **13**, 455 (1974).
- N.T. Yu, B.H. Jo, R.C.C. Chang and J.D. Huber, *Arch. Biochem. Biophys.* **160**, 614 (1974)
- N.T. Yu, *CRC Critical Rev. in Biochem.* **4**, 229 (1977).
- N.T. Yu and C.S. Liu, *J. Amer. Chem. Soc.* **94**, 5127 (1972).
- J. Piatigorsky, J. Horwitz and R.T. Simpson, *Biochim. Biophys. Acta*, **490**, 279 (1977).
- W.S. Duke-Elder, "System of Ophthalmology" Vol. 1, "The Eye in Evolution", p. 399, H. Kimpton, London. 1958.
- E.J. East, R.C.C. Chang, N.T. Yu and J.F.R. Kuck, Jr., *J. Biol. Chem.* **253**, 1436 (1938).
- R. Mathies and N.T. Yu, *J. Raman Spectrosc.* (to be published).
- C.A. Arguello, G.F. Mendes and R.C.C. Leite, *Appl. Opt.* **13**, 1731 (1974).
- R.P. Van Duyne, D.L. Jeanmaire and D.F. Shriver, *Anal. Chem.*, **46**, 213 (1974).
- P.K. Dutta, J.R. Nestor and T.G. Spiro, *Proc. Natl. Acad. Sci.* **74**, 4146 (1977).
- L.A. Carreira, T.C. Maguire and T.B. Malloy, Jr., *J. Chem. Phys.* **66**, 2621 (1977).
- J.J. Song, G.L. Eesley and M.D. Levenson, *Appl. Phys. Lett.* **29**, 567 (1976).
- M.D. Levenson, *Phys. Today*, p. 44 (1977).
- D. Heiman, R.W. Hellwarth, M.D. Levenson and G. Martin, *Phys. Rev. Lett.* **36**, 189 (1976).
- W. Wernicke, A. Lau, M. Pfeiffer, H.J. Weigmann, G. Hunsalz and K. Lenz, *Opt. Commun.* **16**, 128 (1976).
- W. Wernicke, J. Klein, A. Lau, K. Lenz and G. Hunsalz, *Opt. Commun.* **11**, 159 (1974).

\*If this article has aroused your interest, you may wish to refer to "Insight into Eyesight through Resonance Raman." by Aaron Lewis. *THE SPEX SPEAKER*, vol. XXI, No. 2, June 1976.



## from academia to practicalia

The SPEX RAMALOG, laser-Raman spectrophotometer is a sophisticated system designed to reveal esoteric information about the subtle vibrations and rotations swirling through molecules. Right? Well, much of the time. At other times, some very down-to-earth medical and industrial applications prevail.

### Photoluminescent topography

Computer memories, switches, integrated circuits, light emitting diodes, etc.—originating as hundreds of chips from a thin slice of single-crystal silicon, gallium arsenide, or gallium phosphide—demand consistent electrical properties. And an analysis to characterize the wafer material must be nondestructive if the final devices are ever to be fabricated.

M. J. Luciano and D.L. Kingston<sup>1</sup> report an automated luminescent topographic system which does just that for semiconductor wafers—and with a  $10\ \mu\text{m}$  spatial resolution. Of course, it requires a SPEX Double Monochromator. The schematics of the system and a GaAs wafer topograph are illustrated in Fig 1A and B. The considerable luminescence variation indicates epilayer uniformity, or lack of it in this case, and may also be correlated with the practicality of the final device. Whether or not improvement is possible by changing the orientation of the boule in the furnace or some other manufacturing procedure, the ultimate product yield is at stake.

In this fully automated system a  $1\text{W Ar}^+$  laser excites the luminescence, a bidirectional stepper-motor scanner scans the focused laser beam in two orthogonal directions perpendicular to the surface plane of the sample then collects and focuses the luminescent emission into the  $0.85\text{m}$  double spectrometer. A photon counter, desktop calculator and multichannel analyzer detect, handle, and store the data which can be permanently recorded on magnetic tape or plotted for display.

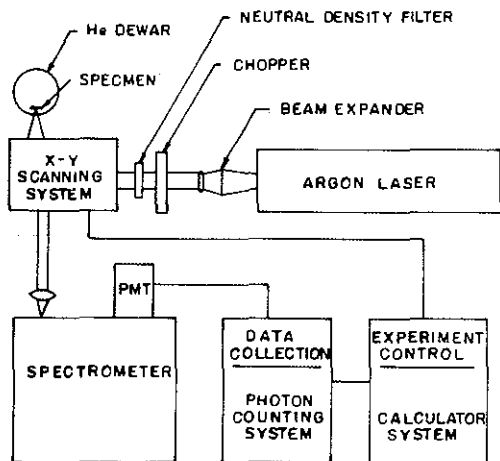


Fig 1A Overall schematic of the topographic system.

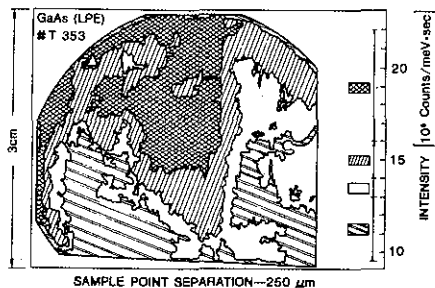


Fig 1B Topographical representation of the epitaxial GaAs surface of a wafer about  $3 \times 3\text{ cm}$ . The shaded bands refer to areas of different intensities of luminescence at around  $1.51\text{ eV}$  ( $821\text{ nm}$ ). This corresponds to the donor-valence transition of the material. According to the authors, "this type of analysis should be useful in predicting which areas of a wafer should produce efficient solid-state devices."

### Monomer-free polymers

A cataract operation entails removal of the lens of the eye. Until very recently results were disheartening. Only narrow-angle vision is attainable with the clumsy, thick glasses proffered; and glasses must be changed to alter the focal distance. One of the happy miracles of our time, however, is that interocular lens implants can now replace nature's own beclouded lenses. Today, a growing group of specialized surgeons delicately suture a tiny polymeric lens inside the eyeball. Afterwards, not only is the angle of vision nearly normal but ordinary bifocal glasses can be worn to correct for reading and distance.

But among the manufacturing challenges to this accomplishment is any monomer retained in the finished product where it can endanger the eye. To monitor production and prevent this possibility, Waters<sup>2</sup> devised a laser-Raman technique for measuring residual methyl methacrylate (MMA) in the polymer (PMMA). Even more recently, in our own laboratory, the detection level has been extended to a few hundredths of a percent (Fig 2). Dr. Waters has also shown, in his work at Brunel Univ., Middlesex, U.K., that the polyvinyl acetate monomer can be quantified in concentrations of 1%; and he predicts the technique to be equally applicable to residual monomers in other polymers.

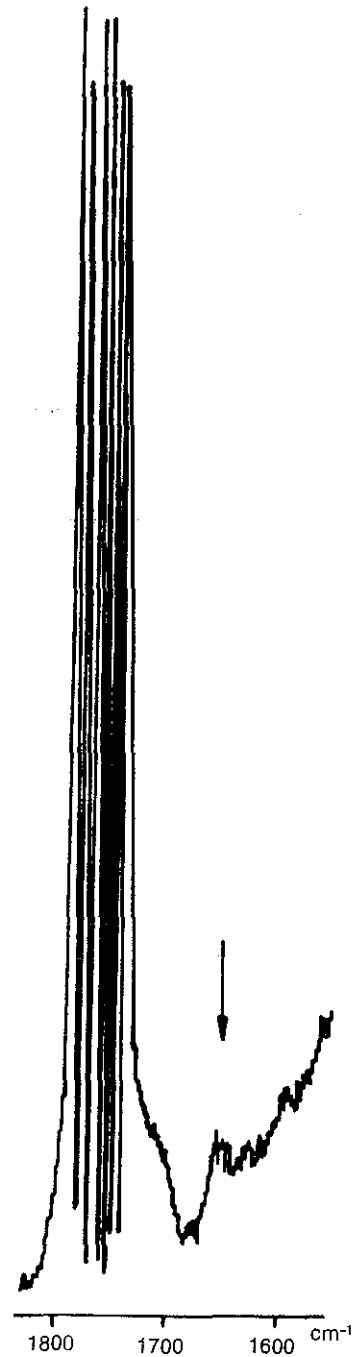


Fig 2 The Raman spectrum of an intraocular lens of PMMA shows a band at around  $1650\text{ cm}^{-1}$  from the monomer at a few hundredths of a percent.

### Hydrogen isotopic alterations revealed

As the lightest of all elements, hydrogen (comprising  $\frac{3}{4}$  of the mass of the known universe) presents a unique isotopic series. Since the hydrogen nucleus consists of only a single proton, the inclusion of a neutron to form deuterium doubles the mass of the atom. Consequently, there is a marked difference between the rotational and vibrational modes of  $H_2$  and  $D_2$ . Hydrogen molecules, however, are homonuclear, diatomic molecules lacking dipole moments. With infrared techniques thus inaccessible, Raman scattering provides a unique window into the  $H_2$  structure. The Raman spectrum in Fig 3 is of the rotation-vibrational modes of  $H_2$ , HD, and  $D_2$  at partial pressures of 2.8, 25, and 70 Torr respectively. The additional mass of the neutron effectively reduces the energy of the rotation-vibrational modes and scattering from hydrogen appears at about  $4180\text{ cm}^{-1}$  while the mixed species appears at  $3650\text{ cm}^{-1}$  and the deuterium, at  $3000\text{ cm}^{-1}$ . A laser line of  $514.5\text{ nm}$  at  $0.9\text{ W}$  and a spectrometer bandpass of  $2.5\text{ cm}^{-1}$  resolved the components of the individual bands which are the fine structure of the Q rotational branch responsible for the transitions. This is most apparent in the band from the more concentrated deuterium. In Fig 4, bandpass was increased to  $37.5\text{ cm}^{-1}$  to integrate the total contribution from  $H_2$ . The area under this curve can provide a quantitative estimate of the specific isotope concentration in the sample.

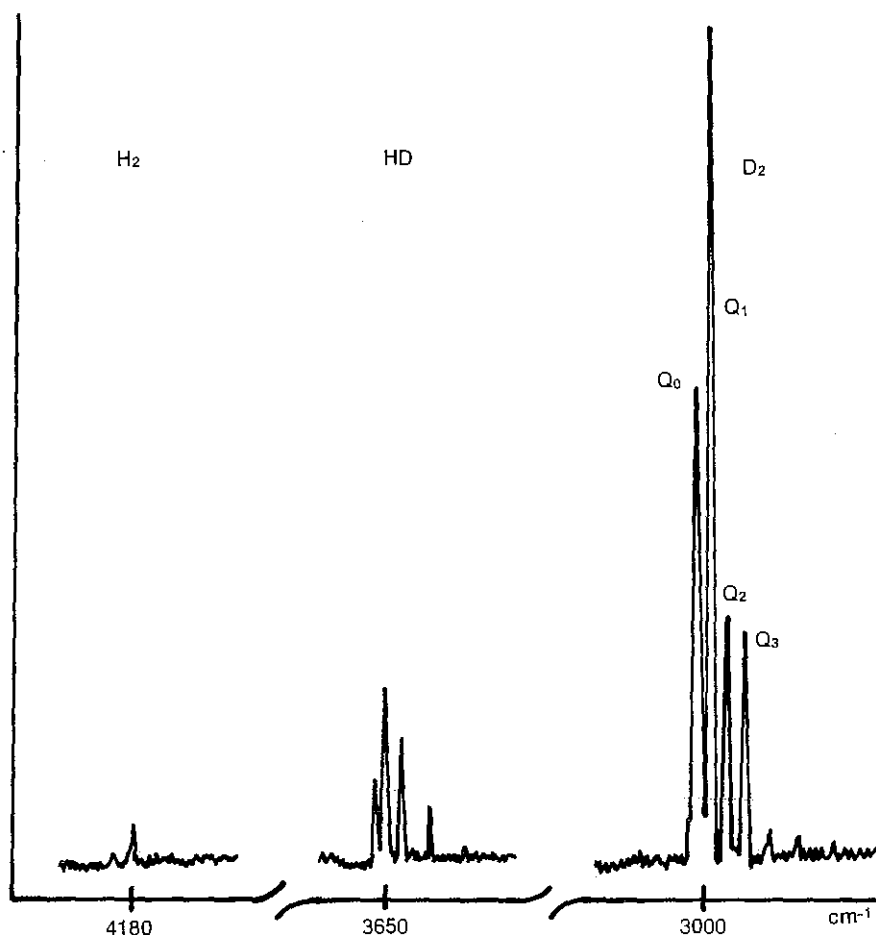


Fig 3 The rotation-vibrational bands of  $H_2$  and  $D_2$  occur at widely different frequencies because the masses of these two isotopes differ so greatly. Differences in the intensities of the peaks are attributable to differences in the partial pressures of the three gases: 2.8, 25, and 70 Torr, respectively, for  $H_2$ , HD, and  $D_2$ .

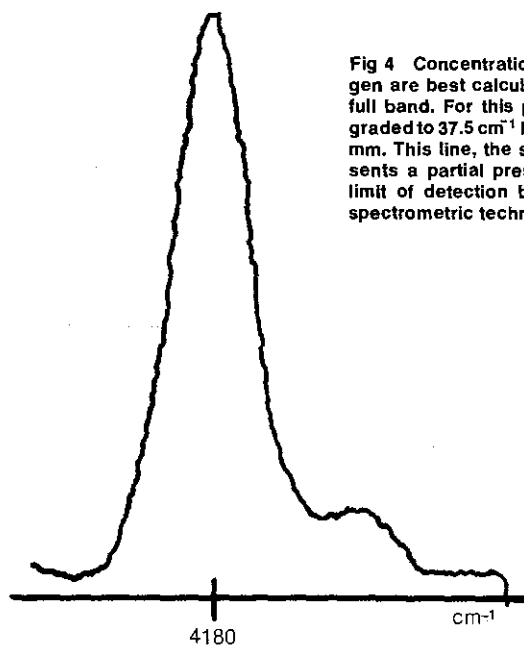


Fig 4 Concentrations of the isotopes of hydrogen are best calculated by integrating over the full band. For this purpose, resolution was degraded to  $37.5\text{ cm}^{-1}$  by widening the slits to a full 3 mm. This line, the same as that in Fig 3, represents a partial pressure of 2.8 Torr, about the limit of detection by more conventional mass spectrometric techniques.

### Characterizing ferric chloride etchants

Ferric chloride baths, etchants for photographic products and printed circuit boards, have been around for a generation, yet they remain notoriously temperamental, especially for etching the fine and still finer lines demanded by solid state miniaturization. As a ferric chloride bath ages, different ions form, interfere, and compete with the main salt. A means of pinning down the reactant species and determining their concentration has been sought and, when all else failed, Raman tried. Still in the preliminary stage, initial results are nonetheless encouraging. Analyses of typical new and used baths show distinct spectral differences both in intensity and position of Raman bands. Some of these bands have already been identified but much more work remains in correlating the species with their effects on etching.

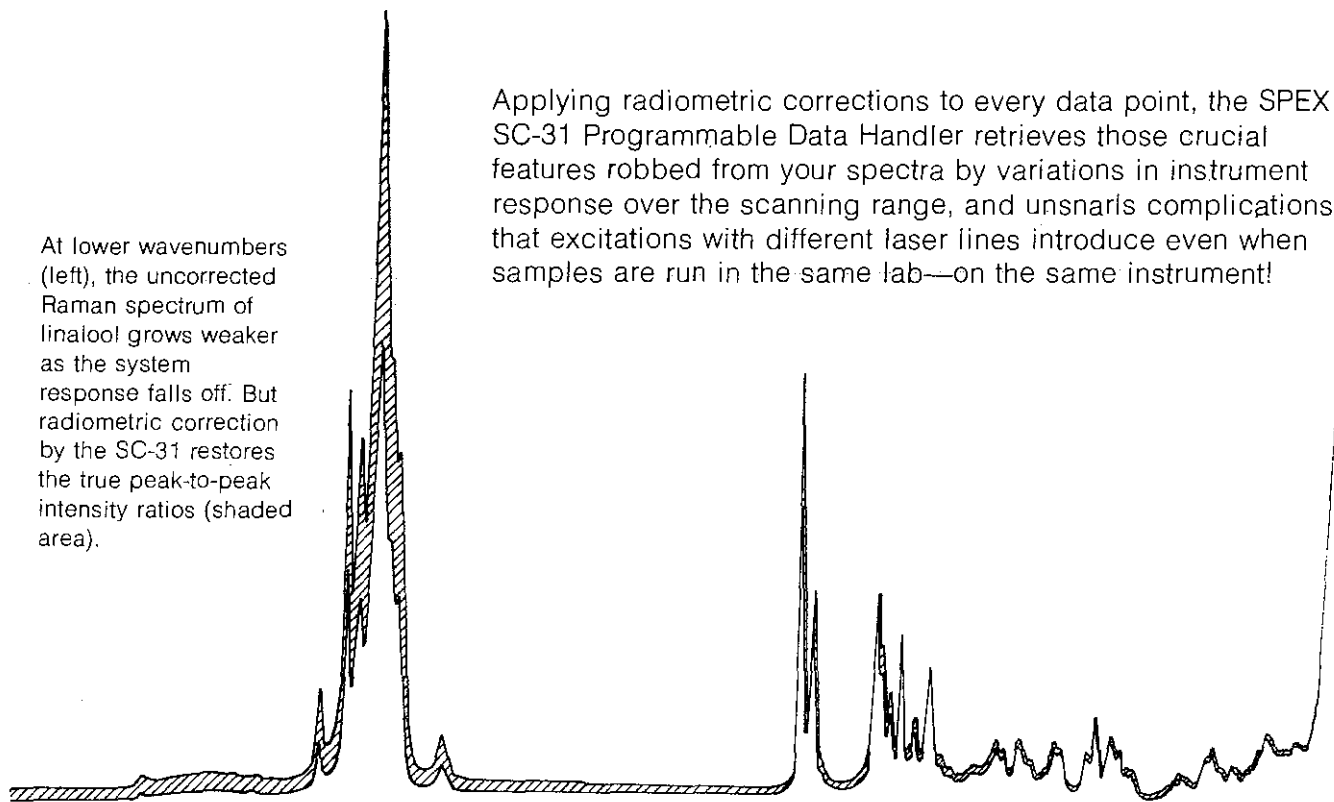
### References

1. M.J. Luciano, D.L. Kingston, *Rev. Sci. Instr.*, **49**, 716, 1978.
2. Waters, D.N., *Proc. 5th Int. Conf. Raman Spectroscopy*, Ferdinand Schulz Verlag, D-7800, "Freiburg IM Breisgau", 500, 1976.

# SOMETHING MISSING

## FROM YOUR RAMAN SPECTRUM M?

At lower wavenumbers (left), the uncorrected Raman spectrum of linalool grows weaker as the system response falls off. But radiometric correction by the SC-31 restores the true peak-to-peak intensity ratios (shaded area).



Applying radiometric corrections to every data point, the SPEX SC-31 Programmable Data Handler retrieves those crucial features robbed from your spectra by variations in instrument response over the scanning range, and unsnarls complications that excitations with different laser lines introduce even when samples are run in the same lab—on the same instrument!

Moreover, the subtraction and signal-averaging prowess of the SC-31 peels away the clutter: background fluorescence and random noise that drape a curtain over Raman bands. Then multiple storage, division, multiplication, integration and other manipulations—all with automatic slewing of the SPEX spectrometer—uncover the feeblest signals.

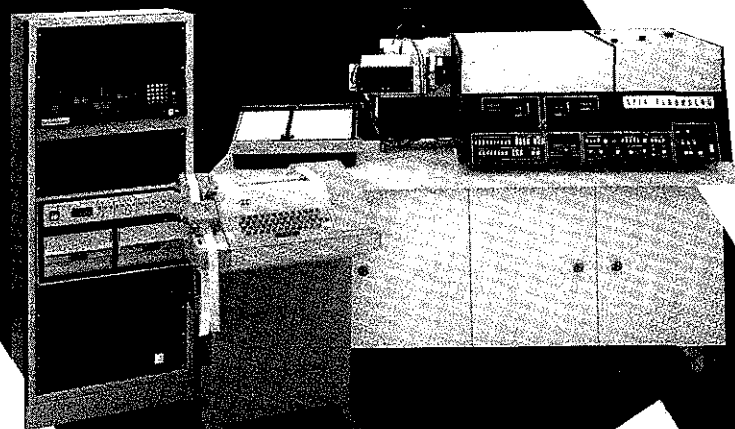
And the list of routines continues to grow. If we neglected to mention your pet function, please ask.

The SC-31 delivers computer performance with a calculator price tag.

# SPEX

## UVISIR® SPECTROMETERS

- WAVELENGTH OR WAVENUMBER READOUT
- FOCAL LENGTHS FROM  $<0.25\text{m TO}> 1.25\text{m}$
- ULTRAVIOLET TO VISIBLE TO INFRARED
- SPEX COMPUDRIVE DIGITAL DRIVE
- SINGLE AND DOUBLE MODELS
- EVACUABLE MODELS
- SCANNING MODELS
- SPECTROGRAPHS



- SC4 SPECTROMETRIC COMPUTER SYSTEM

- TOMCA TELEVISION MULTICHANNEL ANALYZER

- DIGITAL ELECTRONIC ACCESSORIES FOR SPECTROMETER PROGRAMMING, CONTROL, AND READOUT

### FLUOROLOG and FLUOROCOMP

- SPECTROFLUOROMETER SYSTEMS FOR FRONTIER RESEARCH

### RAMALOG and RAMACOMP

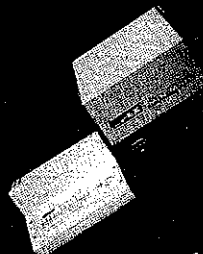
- RAMAN SPECTROPHOTOMETERS UNMATCHED IN PERFORMANCE, VERSATILITY AND RELIABILITY

### GISMO GRAZING INCIDENCE SPECTROMETER/MONOCROMATOR

- FOR PLASMA DIAGNOSTICS

Think  
**BIG**

or  
Think  
**SMALL**



but when you think  
**SPECTROMETER**

Think  
**SPEX**

AMBRIEX S.A.  
Rua Tupi 535, 01233  
Sao Paulo  
BRAZIL

GLEN CRESTON  
16 Carlisle Road  
London, NW9 0HL  
ENGLAND

INSTRUMENTALIA S.R.L.  
P.O.B. 7  
1114 Buenos Aires  
ARGENTINA

QUENTRON OPTICS PTY. LTD.  
576-578 Port Road  
Allenby Gardens  
SOUTH AUSTRALIA 5009

SEISHIN TRADING CO.  
43, Sannomiya-cho  
1-chome, Ikuta-ku  
Kobe, JAPAN

EQUILAB C.A.  
Apartado 60.497  
Caracas 106  
VENEZUELA

HARVIN AGENCIES  
C-7 & 8, Industrial Estate  
Sanantnagar  
Hyderabad -500018 AP INDIA

LANDSEAS (ISRAEL) LTD.  
38, King George Street  
Tel Aviv  
ISRAEL

RADIONICS LTD.  
195 Rue Graveline  
Montreal  
H4T 1R6 CANADA

SPEX INDUSTRIES, GMBH  
Ibherstrasse 53  
D8000 Munchen 83  
WEST GERMANY